JOURNAL OF BACTERIOLOGY, May 1990, p. 2650–2657
0021-9193/90/052650-08$02.00/0

Vol. 172, No. 5

Kinetics of Iron Acquisition from Ferric Siderophores by *Paracoccus denitrificans*

RAYMOND J. BERGERON* AND WILLIAM R. WEIMAR

Department of Medicinal Chemistry, J. Hillis Miller Health Center, University of Florida, Gainesville, Florida 32610-0485

Received 7 August 1989/Accepted 6 January 1990

The kinetics of iron accumulation by iron-starved *Paracoccus denitrificans* during the first 2 min of exposure to ^{55}Fe-labeled ferric siderophore chelates is described. Iron is acquired from the ferric chelate of the natural siderophore L-parabactin in a process exhibiting biphastic kinetics by Lineweaver-Burk analysis. The kinetic data for 1 μM < [Fe L-parabactin] < 10 μM fit a regression line which suggests a low-affinity system (K_m = 3.9 ± 1.2 μM, V_{max} = 494 pg-atoms of ^{55}Fe min^{-1} mg of protein^{-1}), whereas the data for 0.1 μM ≤ [Fe L-parabactin] ≤ 1 μM fit another line consistent with a high-affinity system (K_m = 0.24 ± 0.06 μM, V_{max} = 108 pg-atoms of ^{55}Fe min^{-1} mg of protein^{-1}). The K_m of the high-affinity uptake is comparable to the binding affinity we had previously reported for the purified ferric L-parabactin receptor protein in the outer membrane. In marked contrast, ferric D-parabactin data fit a single regression line corresponding to a simple Michaelis-Menten process with comparatively low affinity (K_m = 3.1 ± 0.9 μM, V_{max} = 125 pg-atoms of ^{55}Fe min^{-1} mg of protein^{-1}). Other catecholamide siderophores with an intact oxazoline ring derived from L-threonine (L-homoparabactin, L-agrobactin, and L-vibriobactin) also exhibit biphasic kinetics with a high-affinity component similar to ferric L-parabactin. Circular dichroism confirmed that these ferric chelates, like ferric L-parabactin, exist as the Λ enantiomers. The A forms of ferric parabactin (ferric D- and L-parabactin A), in which the oxazoline ring is hydrolyzed to the open-chain threonyl structure, exhibit linear kinetics with a comparatively high K_m (1.4 ± 0.3 μM) and high V_{max} (324 pg-atoms of ^{55}Fe min^{-1} mg of protein^{-1}). Furthermore, the marked stereospecificity seen between ferric D- and L-parabactins is absent; i.e., iron acquisition from ferric parabactin A is nonstereospecific. The mechanistic implications of these findings in relation to a stereospecific high-affinity binding followed by a nonstereospecific postreceptor processing is discussed.

The gram-negative soil bacterium *Paracoccus denitrificans* excretes a hexacoordinate catecholamide iron chelator, a siderophore, parabactin (Fig. 1) (36, 42). The five aromatic hydroxyls and the oxazoline ring nitrogen of this ligand have been implicated as the donor centers coordinated to iron in the ferric L-parabactin–chelate complex (34). Previously we demonstrated that the kinetics of iron incorporation by *P. denitrificans* grown in iron-deficient media is consistent with an "iron taxi" mechanism (4). In the mechanism envisaged, the ferric siderophore binds to a specific receptor protein in the outer membrane, with subsequent release of iron from the siderophore complex while still on the extracellular side of the inner cytoplasmic membrane. The released iron is then transported into the cell, while the deferrated ligand remains extracellular where it may be reused for iron transport. We have identified, isolated, and partially purified a stereospecific high-affinity receptor for ferric L-parabactin in the *P. denitrificans* outer membrane (10).

Our current studies are aimed at understanding and defining the steps involved in processing the complex between initial binding to the receptor and final delivery of iron to the cytoplasm. This report examines the kinetics of iron acquisition from ^{55}Fe-labeled ferric siderophores by iron-starved *P. denitrificans*. The chirality of the ferric chelates of several natural and synthetic siderophores is determined by circular dichroism and related to the kinetic findings. We confirm the presence of a high-affinity transport system for ferric L-parabactin with an apparent K_m of 0.24 ± 0.06 μM. A comparison of the kinetics of ferric L- and D-parabactin reveals a striking stereospecificity for iron uptake. Only ferric siderophores with an intact oxazoline ring derived from L-threonine and forming the Λ chelate enantiomer are recognized by the high-affinity system. Although *P. denitrificans* very effectively acquires iron from ferric L-parabactin A, it does not use a high-affinity system. Surprisingly, ferric D-parabactin A is equally effective. We suggest that this might reflect a nonstereospecific component in ferric L-parabactin processing, an apparatus normally acting at a stage after the stereospecific high-affinity binding to the outer membrane receptor.

MATERIALS AND METHODS

Materials. $^{55}FeCl_3$ (specific activity, 43.57 Ci g^{-1}) in 0.5 M HCl and Biofluor Scintillation Cocktail were purchased from Du Pont, NEN Research Products. Desferrioxamines B and E were gifts from CIBA-GEIGY Corp. L-Agrobactin (8), L-agrobactin A (9), L-homoparabactin (6), and L-vibriobactin (5) were synthesized as previously reported. D-Parabactin and D-parabactin A were synthesized and purified in a manner identical to that for the corresponding L-enantiomers, but with *N-tert*-butoxycarbonyl-D-threonine (BOC-D-Thr) instead of BOC-L-Thr (3, 4). UV-visible spectra were obtained on a Shimadzu spectrophotometer, optical rotations were measured on a JASCO DIP-360 polarimeter, and circular dichroism spectra were determined on a JASCO J-500 CD spectropolarimeter.

Preparation of siderophore chelates. All solutions and solvents were purged with nitrogen or argon prior to use. The ferric chelates of desferrioxamines B and E were prepared by addition of an $FeCl_3$ stock solution in 0.1 N HCl

* Corresponding author.

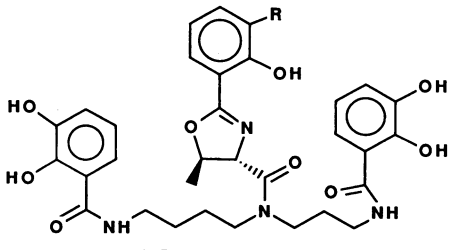

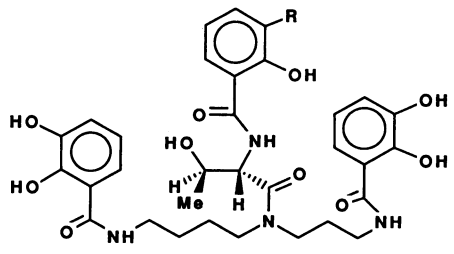

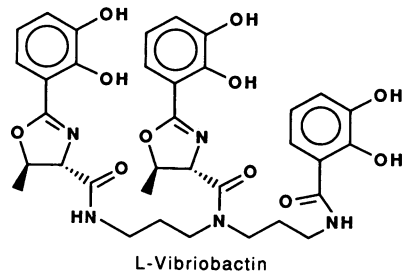

FIG. 1. Structure of catecholamide siderophores used in this study. L-Parabactin and L-agrobactin are naturally occurring siderophores which contain a spermidine backbone and an oxazoline ring with two asymmetric carbons derived from L-(2*S*,3*R*)-threonine. The synthetic analog D-parabactin, prepared from D-(2*R*,3*S*)-threonine, and the homolog L-homoparabactin, in which the aminopropyl portion of spermidine is elongated by one carbon to give the bis(4-aminobutyl)amine, homospermidine, are also addressed in this communication. Hydrolysis of the oxazoline ring yields the A-forms, with an open-chain threonyl residue. L-Vibriobactin, produced by *Vibrio cholerae*, contains a norspermidine backbone (i.e., the aminobutyl portion of spermidine is shortened by one carbon) and two oxazoline rings derived from L-threonine. We have also examined two hexacoordinate hydroxamate siderophores (not shown), desferrioxamine B (a linear molecule), and desferrioxamine E (nocardamine; a cyclic hydroxamate) for iron transport activity in *P. denitrificans*.

to a 10% molar excess of ligand followed by immediate adjustment of the pH to 7.4 with Tris. Ferric nitrilotriacetate [ferric$(NTA)_2$] was prepared by addition of 2.2 volumes (10% excess) of 30 mM trisodium NTA to 1 volume of 30 mM $FeCl_3$ stock solution in 0.1 N HCl followed by immediate adjustment of the pH to 7.0 with 500 mM Tris hydrochloride to give a final stock concentration of 5 mM ferric$(NTA)_2$. Ferric acetoacetonate [ferric$(AcAc)_3$] was prepared by shaking 1 volume of 5 mM $FeCl_3$ in 0.01 N HCl with one volume of 15 mM acetylacetone in ethyl acetate. One volume of 100 mM ammonium bicarbonate was added, and the mixture was shaken again. The orange-red organic layer containing ferric$(AcAc)_3$ was twice washed with an equal volume of water. The ferric chelates of the catecholamides were prepared by ligand exchange with either ferric$(NTA)_2$ or ferric$(AcAc)_3$. In the former case, a 10% molar excess of catecholamide in ethanol ($\leq$50 μl) was added to 5 mM ferric$(NTA)_2$ followed by sufficient 500 mM Tris hydrochloride (pH 7.4) to give a 300 μM ferric catecholamide solution.

The chelate was then purified on a short column of C_{18} silanol reversed-phase chromatographic support (J. T. Baker Chemical Co.). The column had been first washed with iron-free ethanol, followed by distilled-deionized water, and 500 mM Tris hydrochloride (pH 7.4). The chelate solution (e.g., 1 to 5 ml of 200 to 300 μM chelate) was then applied to the column, followed by washes with several column volumes of 500 mM Tris hydrochloride (pH 7.4) and distilled water. The chelate remained at the top of the column as a purple band, which was then eluted as a tight band on application of 200 μl of ethanol followed by 500 μl of water. The purple eluate was collected, the ethanol was removed in a stream of nitrogen, and the final concentration was adjusted to 100 to 300 μM with 100 mM Tris hydrochloride (pH 7.4). Ferric catecholamides were also readily prepared by addition of a 10% molar excess of ligand in ethyl acetate to a 4 mM ferric$(AcAc)_3$ solution in ethyl acetate. This solution was shaken with a small volume of 100 mM Tris hydrochloride (pH 7.4). The aqueous layer became a deep wine-purple color during the next several minutes. The organic layer was discarded, and the aqueous chelate was washed three times with ethyl acetate. The chelates were then chromatographed on a short C_{18} silanol reversed-phase support as described above. Yields were essentially quantitative. Circular dichroism (CD) spectra revealed no racemization during the preparation of catecholamide chelates by either the NTA or AcAc methods. Radiolabeled chelates were prepared in exactly the same manner, except that the iron stock solution was [^{55}Fe]ferric chloride in 0.5 M HCl. Specific activities ranged from undiluted isotope at 43.57 Ci g of Fe^{-1} to preparations diluted 2- to 10-fold with cold isotope.

The C_{18} reversed-phase column purification gave chelate solutions which were shown by thin-layer chromatography to be essentially free of excess ligand. Polyethyleniminecellulose was cut into 100-mm strips, preequilibrated with running buffer, air dried before use, and eluted with freshly prepared tetrahydrofuran–methanol–10 mM tetrabutylammonium phosphate (pH 7.0) (2:2:1). In this system, free catecholamide ligands (i.e., parabactin, homoparabactin, agrobactin, vibriobactin, agrobactin A, and parabactin A) migrated close to the solvent front (R_f = 0.92-0.97). The ferric chelates of those ligands with intact oxazoline rings moved as red-violet spots with R_fs of 0.59 to 0.62 (ferric parabactin, ferric homoparabactin), 0.60 to 0.64 (ferric agrobactin), and 0.63 to 0.71 (ferric vibriobactin), whereas ferric parabactin A (purple, R_f = 0.03 to 0.04) and ferric agrobactin A (red-violet, R_f = 0.02 to 0.03) moved only slightly. This thin-layer chromatography system allowed us to assess the magnitude of ligand-metal exchange occurring during the time frame of our uptake experiments (2 min). As an example, 5 μl of 100 μM [^{55}Fe]ferric L-parabactin A in 100 mM Tris hydrochloride (pH 7.4) was mixed with 5 μl of 250 μM L-parabactin in methanol and, either immediately for a zero time assessment or after a 2-min incubation, spotted on a thin-layer chromatography strip and developed. The developed thin-layer chromatography strip was then cut into 0.5-cm segments, which were analyzed for radioactivity by liquid scintillation counting. In the latter case, only the segments corresponding to ferric L-parabactin A contained about 94% of the applied radiolabel and the segments corre-

sponding to ferric L-parabactin contained about 4.7% of the applied radiolabel. When the mixture was spotted immediately, the corresponding values were 97.4 and 1.5%, respectively.

The final concentration of all chelates was confirmed spectrophotometrically prior to use: ferrioxamine B ($\varepsilon_{428\ nm} = 2.8 \times 10^3\ M^{-1}\ cm^{-1}$) (48), ferrioxamine E ($\varepsilon_{428\ nm} = 2.8 \times 10^3\ M^{-1}\ cm^{-1}$), ferric agrobactin ($\varepsilon_{507\ nm} = 3.6 \times 10^3\ M^{-1}\ cm^{-1}$), ferric agrobactin A ($\varepsilon_{495\ nm} = 3.65 \times 10^3\ M^{-1}\ cm^{-1}$), ferric homoparabactin ($\varepsilon_{520\ nm} = 3.1 \times 10^3\ M^{-1}\ cm^{-1}$), ferric parabactin ($\varepsilon_{516\ nm} = 3.1 \times 10^3\ M^{-1}\ cm^{-1}$), ferric parabactin A ($\varepsilon_{522\ nm} = 3.32 \times 10^3\ M^{-1}\ cm^{-1}$), and ferric vibriobactin ($\varepsilon_{496\ nm} = 3.4 \times 10^3\ M^{-1}\ cm^{-1}$).

Protein determination. The protein concentration was estimated by using bovine serum albumin as the standard by the method of Lowry et al. (29) with modifications for membrane protein samples as described by Markwel et al. (30). The cell density was estimated from turbidometric optical density at 660 nm (OD_{660}) with dilutions in transport buffer as required to keep in the linear range ($OD_{660} < 2.00$). One OD_{660} unit refers to the amount of cells producing an optical density of 1.000 when suspended in transport buffer at room temperature. Under our typical growth conditions, 1 OD_{660} unit corresponded to ca. 0.25 mg of protein.

Low-iron defined minimal salts medium. To obtain productive growth of *P. denitrificans* under controlled low-iron stress, it was necessary to take vigorous steps to remove all the iron (present as contaminants of reagent grade chemicals). For a 12-liter batch, 70.8 g of succinic acid, 48.0 g of KH_2PO_4, 60.6 g of NaH_2PO_4, and 19.2 g of NH_4Cl were dissolved in 10 liters of glass-distilled deionized water. This solution, pH ca. 4.5, was autoclaved and allowed to sit at 4°C for 3 to 4 days to allow iron salts to coagulate (40). The solution was filtered through a 0.2-μm membrane and, after the pH had been adjusted to 7.0, was passed through a column of 1,500 g of Chelex 100 resin (Bio-Rad Laboratories). The pH was again adjusted to 7.0, 300 ml of Chelex-treated 20% Tween 80 solution was added to prevent clumping of cells, and the final volume was adjusted to 12 liters (final Tween concentration, 0.5%). Since the above treatments remove other trace elements and divalent cations in addition to iron, these components were added as a supplement following the Chelex column treatment so that complete minimal salts medium contained an optimized mixture of trace elements: $MgSO_4$ (1.7 mM), Ca^{2+} (182 μM), Mn^{2+} (10 μM), Zn^{2+} (1 μM), Cu^{2+} (0.1 μM), and Co^{2+} (0.01 μM). The degree of low-iron stress could then be carefully controlled by addition of a known quantity of ferric$(NTA)_2$ (0 to 1.0 μM).

Bacterial strain and culture conditions. *P. denitrificans* ATCC 17741 was maintained on Trypticase soy agar plates (BBL Microbiology Systems). Individual colonies were inoculated into 20 ml of Trypticase soy broth (BBL) (4) and incubated with rotary shaking for 24 h at 30°C. Inoculations were then made from this culture into 50 ml of minimal salts liquid medium containing 1 μM Fe[III] to give a starting OD_{660} of 0.015 and incubated with shaking at 30°C for 16 h. This culture was then used to inoculate a 250-ml culture flask of 50 ml of minimal salts medium containing 0.5 μM Fe(III) to give a starting OD_{660} of 0.040. The flask was incubated with shaking (120 rpm) at 30°C for 12 h. At the end of this incubation, the cells were in late log growth (OD_{660} = 3.0 to 3.5; growth rate proportional to $10^{0.16t}$, where t is time in hours) and the medium was positive for catechols ($OD_{515} >$ 0.100) when estimated by a modification of the nitrosomolybdate method of Arnow (13). Sodium dodecyl sulfate-polyacrylamide gel electrophoresis of representative cultures showed that under these conditions the iron-regulated 80-kilodalton polypeptides were induced (10, 20, 44). We have previously shown an outer membrane ferric L-parabactin receptor to be among these iron-regulated proteins (10). The cells were then prepared for transport assay by centrifugation at 15 to 20°C followed by washing with iron-free minimal salts medium (transport buffer) at 15 to 20°C. The washed pellet was then suspended in transport buffer to OD_{660} = 1.000.

Transport assay. Polystyrene conical-bottom tubes (50 ml) were used as assay incubation vessels. The tubes, each containing 3.45 ml of cell suspension (OD_{660} = 1.000) were incubated with shaking in a water bath at 30°C for 15 min. The assays were initiated by addition of 50 μl of radiolabeled chelate. Portions (500 μl) were withdrawn every 20 s for 2 min. The transport reaction was stopped by adding the portion to 5 ml of prechilled (O°C) transport buffer. Whatman GF/F fiber glass filters, which had been presoaked for 24 h in 500 μM unlabeled chelate and rinsed with 5 ml of chilled transport buffer, were used to separate cells from external medium by rapid filtration. After two rinses with 5 ml of chilled transport buffer, the filters were dried at 70°C and placed in a scintillation vial with 10 ml of Biofluor. Triplicate 100-μl portions of each incubation mixture were counted to verify the total amount of label added. Cell-associated radioactivity was measured by liquid scintillation counting.

The six datum points taken during the first 2 min for each assay tube were fitted to a regression line with a slope equal to the initial reaction velocity (v_0). These initial rates, expressed as picogram-atoms of ^{55}Fe per minute per milligram of protein, were then used to generate Lineweaver-Burk plots by using Celand's Fortran program (12) to estimate K_m, V_{max}, and their standard errors. Rates varied linearly with the number of cells present from OD_{660} values of 0.500 to 2.000. All data were corrected for cell growth during the assay period. Since there was modest variation in transport competence among culture batches, all data were normalized to [^{55}Fe]ferric L-parabactin for comparison purposes. Thus, every experiment included an estimate of v_0 for [^{55}Fe]ferric L-parabactin at 1 μM, and all data were normalized to V_0 = 106.8 pg-atoms of ^{55}Fe = min^{-1} mg of $protein^{-1}$ for 1 μM [^{55}Fe]ferric L-parabactin.

RESULTS AND DISCUSSION

The stereospecificity of ferric parabactin transport in *P. denitrificans* is illustrated in Fig. 2. Iron accumulation data from [^{55}Fe]ferric D-parabactin fit a straight-line Lineweaver-Burk reciprocal plot and thus obey a simple Michaelis-Menten model. Even at high concentrations, ferric D-parabactin is a poor iron source for *P. denitrificans* compared with ferric L-parabactin, as indicated by V_{max} for iron accumulation (Table 1). The stereospecific differences in uptake rates are pronounced at ligand concentrations below 1 μM, reflecting the presence of a high-affinity transport system for ferric L-parabactin.

An enlargement of Fig. 2 indicates the ferric L-parabactin data are nonlinear (Fig. 3) and apparently biphasic. If analyzed separately, the data for 1 μM < [L-parabactin] < 10 μM fit one line (r = 0.991), suggesting a low-affinity system (K_m = 3.9 ± 1.2 μM), while the data for 0.1 μM ≤ [L-parabactin] ≤ 1 μM fit another line (r = 0.996) consistent with a high-affinity system (K_m = 0.24 ± 0.06 μM). The apparent K_m of the high-affinity uptake is comparable to the

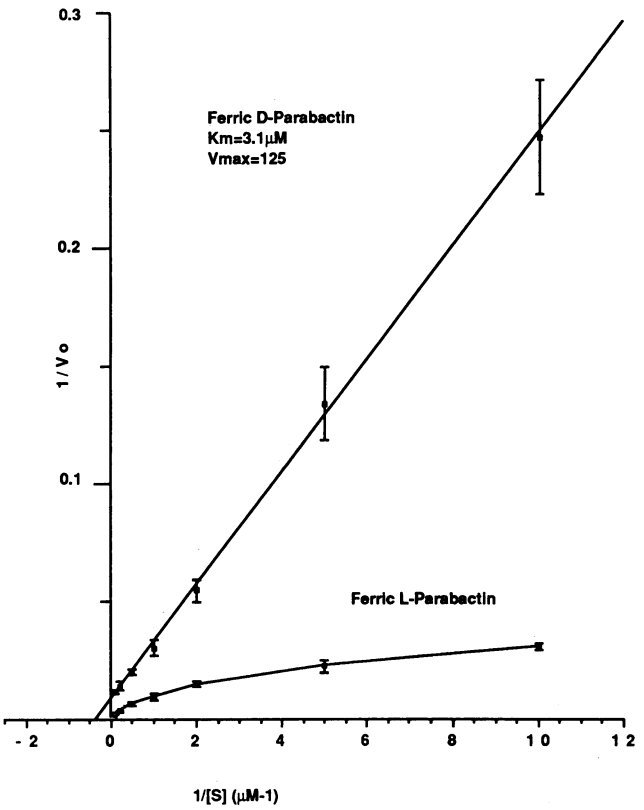

FIG. 2. Lineweaver-Burk plot of kinetic data for the transport of [^{55}Fe]ferric D-parabactin and [^{55}Fe]ferric L-parabactin for 0.1 μM ≤ [S] ≤ 10 μM, where [S] is the concentration of chelate added to external medium at t = 0. The D-parabactin data in this and other experiments can be fitted on a single regression line (r = 0.999) corresponding to a simple Michaelis-Menten process with comparatively low affinity (K_m = 3.1 ± 0.9 μM; V_{max} = 125 ± 11 pg-atoms of ^{55}Fe min^{-1} mg of protein^{-1}). The L-parabactin data are nonlinear (see Fig. 3), but if analyzed separately, the data for 1 μM < [L-parabactin] < 10 μM fit one line (r = 0.991), suggesting a low-affinity system (K_m = 3.9 ± 1.2 μM; V_{max} = 495 ± 41 pg-atoms of ^{55}Fe min^{-1} mg of protein^{-1}), while the data for 0.1 μM ≤ [L-parabactin] ≤ 1 μM fit another line (r = 0.996), consistent with a high-affinity system (K_m = 0.24 ± 0.06 μM; V_{max} = 118 ± 19 pg-atoms of ^{55}Fe min^{-1} mg of protein^{-1}). Note that the data in these two concentration ranges are analyzed independently; i.e., the high-affinity data are not corrected for contributions made by the low-affinity system operating at [S] < 1 μM, nor are the low-affinity data corrected for contributions made by the high-affinity system operating at [S] > 1 μM. Data are presented as means of four (D-parabactin) or five (L-parabactin) determinations and standard deviations (bars) for [S] = 0.1, 0.2, 0.5, 1.0, 2.0, 5.0, and 10.0 μM.

binding affinity we had previously reported for the purified ferric L-parabactin receptor protein in the outer membrane (10). The K_m value of 0.24 μM for high-affinity ferric L-parabactin transport in *P. denitrificans* compares with the K_ms reported for high-affinity transport systems for ferrichrome (0.15 to 0.25 μM) and ferric enterobactin (0.10 to 0.36 μM) in *Escherichia coli* (18, 33, 43). The K_ms reported for siderophore-mediated iron transport in other microorganisms range from an extremely high-affinity system (K_m = 0.04 μM) for ferric schizokinen transport in the cyanobacterium *Anabaena* sp. (26) to comparatively low-affinity systems such as that for ferric coprogen transport (K_m = 5 μM) in *Neurospora crassa* (22, 46).

A parabactin homolog and two analogs with an intact oxazoline ring derived from L-threonine (i.e., L-homoparabactin, L-agrobactin, and L-vibriobactin) (Fig. 1) also exhibit biphasic kinetics with a high-affinity component (K_m = 0.13 to 0.26 μM), similar to ferric L-parabactin (Table 1). The ferric chelates of these L-parabactin analogs (0.5 and 1.0 μM) inhibit accumulation of ^{55}Fe from [^{55}Fe]ferric L-parabactin with simple substrate-competitive Michaelis-Menten kinetics for 0.1 μM ≤ [S] ≤ 1.0 μM and K_is of 0.4 ± 0.09 μM (L-homoparabactin), 0.29 ± 0.13 μM (L-agrobactin), and 0.15 ± 0.11 μM (L-vibriobactin). In the reverse experiment, ferric L-parabactin (0.5 and 1.0 μM) is a substrate-competitive inhibitor of [^{55}Fe]ferric L-vibriobactin transport (K_i = 0.28 ± 0.08 μM). Ferric D-parabacatin (0.5 and 1.0 μM) has no effect on [^{55}Fe]ferric L-parabactin transport except at very high concentrations (≥10 μM ferric D-parabactin). Thus, the high-affinity ferric L-parabactin receptor appears to recognize and allows acquisition of iron from all these ferric L-oxazoline homologs, at least for 0.1 μM ≤ [S] ≤ 1.0 μM. The degree to which this system also contributes to the low-affinity phase (1 μM ≤ [S] ≤ 10 μM) of the biphasic kinetic profile is less clear. Biphasic kinetics have been observed for a number of membrane transport systems. In some cases the presence of two independent systems for transport of the same substrate explains the observed kinetics (16). Alternatively, negative allosteric interactions can result in a system with a low K_m at low [S], which converts to a high-K_m system at high [S] (17, 21). These questions, including the possibility of allosteric regulation of iron transport in *P. denitrificans*, are subjects of ongoing investigation in our laboratory.

The fact that all the ferric catecholamides tested which had L-oxazoline rings exhibited biphasic kinetics with a high-affinity component, while the D-oxazoline analog, ferric D-parabactin, displayed marked kinetic differences including a lack of a high-affinity component, prompted us to further investigate potential contributions of molecular dissymmetry to these distinctive kinetic features. The similarities in ring size and nature of the chelate donor centers in parabactin and its homologs allow direct comparison of their CD spectra with those of ferric hydroxamate and catecholate chelates of known absolute configuration (11, 23, 38).

The positive CD band maxima ($\Delta\varepsilon$ = +2.2 at 550 nm) associated with the low-energy transition in the visible spectrum (Fig. 4, insert) of ferric L-parabactin (λ_{max} = 516 nm) is characteristic of the Λ chelate enantiomer. This is in agreement with a previous report of the CD spectrum of ferric L-parabactin (34) and with high-field nuclear magnetic resonance nmr studies of gallium(III) L-parabactin (3). Our CD data (not shown; to be detailed in a separate report) indicate that the other ferric catecholamides containing an oxazoline ring derived from L-threonine (i.e., L-agrobactin, L-homoparabactin, and L-vibriobactin) all exist in solution as the Λ chelate enantiomers, while ferric D-parabactin is the mirror-image Δ chelate enantiomer (Fig. 4). Thus, these chelates, like ferric L-parabactin, differ from ferric D-parabactin at three chiral centers: two asymmetric carbons in the oxazoline ring derived from D-(2*R*,3*S*)-threonine (D-parabactin) and L-(2*S*,3*R*)-threonine (L-parabactin, as well as metal center chiral configuration. (L-Vibriobactin contains two oxazoline rings [Fig. 1] and thus has four asymmetric carbons.)

Although *P. denitrificans* does not produce or secrete hydroxamate siderophores, it is able to accumulate ^{55}Fe from the hydroxamate siderophore complexes [^{55}Fe]ferrioxamine B and [^{55}Fe]ferrioxamine E (nocardamine) by low-affinity, low-V_{max} transport mechanisms when compared

TABLE 1. Iron accumulation kinetic data

Chelate[a]	Kinetics	K_m[b]	V_{max}[c]
Ferric L-parabactin (5)	Bimodal	0.24 ± 0.06 μM (high affinity)	118 ± 19
		3.9 ± 1.2 μM (low affinity)	495 ± 41
Ferric L-homoparabactin (2)	Bimodal	0.26 ± 0.10 μM (high affinity)	142 ± 24
		2.6 ± 1.3 μM (low affinity)	254 ± 31
Ferric L-vibriobactin (3)	Bimodal	0.18 ± 0.07 μM (high affinity)	72 ± 16
		5.8 ± 1.4 μM (low affinity)	544 ± 51
Ferric L-agrobactin (3)	Bimodal	0.13 ± 0.08 μM (high affinity)	46 ± 8
		1.6 ± 0.8 μM (low affinity)	221 ± 18
Ferric D-parabactin (4)	Linear	3.1 ± 0.9 μM	125 ± 11
Ferric L-parabactin A (4)	Linear	1.4 ± 0.3 μM	324 ± 21
Ferric D-parabactin A (2)	Linear	1.3 ± 0.3 μM	330 ± 12
Ferrioxamine B (3)	Linear	33 ± 9.3 μM	98 ± 16
Ferrioxamine E (2)	Linear	26 ± 6.1 μM	7.6 ± 2.1

[a] Number in parentheses refers to the number of assays at each chelate concentration (i.e., 0.1, 0.2, 0.5, 1.0, 2.0, 5.0, and 10 μM for most chelates, 0.1, 0.25, 0.5, 1.0, 2.0, 5.0, and 10 μM for ferric L-parabactin A and ferric D-parabactin A, and 0.1, 0.25, 0.5, 1.0, 2.0, 5.0, 10, and 20 μM for ferrioxamines B and E).
[b] K_m ± standard error determined as described in Materials and Methods.
[c] Picogram-atoms of ^{55}Fe per minute per milligram of protein (± standard error).

with ^{55}Fe accumulation from [^{55}Fe]ferric L-parabactin or [^{55}Fe]ferric parabactin A (Table 1). Many microorganisms are able to acquire iron from exogenous siderophores and sometimes produce specific membrane receptors to recognize and transport these complexes (2, 15, 18, 22, 32, 47). However, we currently have no evidence to indicate the presence of such specific hydroxamate siderophore transport systems in *P. denitrificans*. Although the possibility of iron acquisition by a ligand-metal exchange mechanism from these ferric hydroxamates cannot be absolutely excluded, it seems unlikely that free parabactin produced by the cell is involved in ferrihydroxamate deferration, in spite of a formation constant which strongly favors ferric L-parabactin (K_f = ca. 10^{48} [34]) over ferrioxamine B ($K_f = 10^{30.6}$ [48]) or ferrioxamine E ($K_f = 10^{32.5}$ [1]) on thermodynamic grounds. We monitored ligand-metal exchange between ferrioxamine B and parabactin as well as between ferrioxamine B and parabactin A by spectrophotometrically recording the red-violet catecholamide-iron absorption band ($\lambda_{max} \approx 520$ nm). The exchange reaction was initiated by charging a cuvette with a 50% methanolic solution of 350 μM ferrioxamine B, either 300 μM L-parabactin or 300 μM L-parabactin A, and 25 mM Tris hydrochloride (pH 7.4). If the reaction is allowed to proceed to equilibrium (5 days to be certain of completion; 99% of the equilibrium value had been achieved for ferric L-parabactin after 12 h), essentially all the L-parabactin (>99.5%) is in the ferric form, while only about 32% of L-parabactin A is in the form of ferric L-parabactin A, consistent with the exceptionally high stability constant of ferric L-parabactin (34). However, these appear to be kinetically slow processes. During the first 10 min, 0.13 to 0.2% of free ligand present is converted to ferric parabactin or ferric parabactin A per min. Even after 5 min, less than 1% of iron exchange had occurred. Since the ligand and chelate concentrations in the assay are considerably lower than the 300 and 350 μM present in this exchange experiment, even lower exchange rates are expected under assay conditions. Thus, at least under these conditions, the kinetics of ligand-metal interchange between parabactin and ferric hydroxamate seem too slow to account for the accumulation of ^{55}Fe from the hydroxamate siderophore complexes observed during the 2-min duration of a transport experiment.

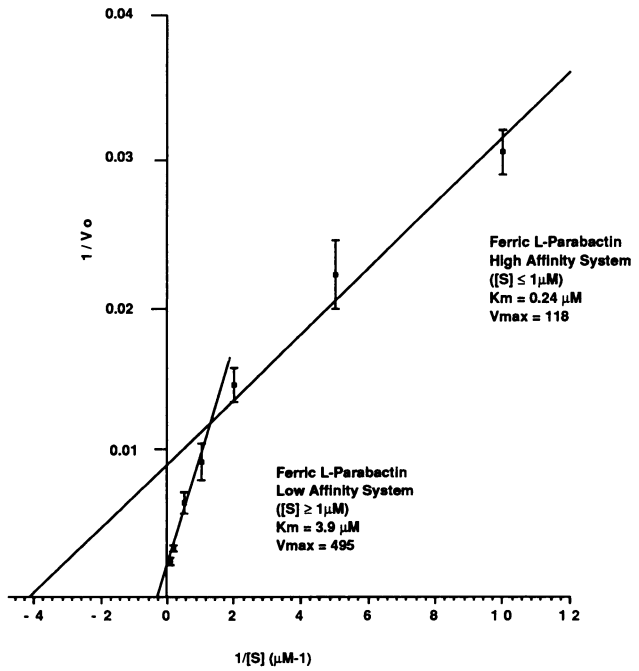

FIG. 3. Enlarged view of [^{55}Fe]ferric L-parabactin kinetic data presented in Fig. 2, emphasizing the bimodal nature of this plot. The data for 0.1 μM ≤ [L-parabactin] ≤ 1 μM and the data for 1 μM ≤ [L-parabactin] ≤ 10 μM are fitted to regression lines respectively representing high- and low-affinity phases of uptake. Data are presented as means of five determinations and standard deviations (bars) for [S] = 0.1, 0.2, 0.5, 1.0, 2.0, 5.0, and 10.0 μM.

As described above, only chelates with 2-oxazoline rings derived from L-threonine appear to exhibit biphasic iron transport kinetics in *P. denitrificans*. A number of siderophores containing 2-oxazoline systems have been characterized. In addition to L-agrobactin (35), L-parabactin (36, 42), and L-vibriobactin (19), all members of the mycobactin family contain a 2-oxazoline derived from either L-threonine or L-serine (41). In addition, pyochelin (14) and anguibactin (24) contain the closely related 2-thiazoline ring derived from L-cysteine. The chemistry of the 2-oxazoline system may confer on these siderophores special properties of biological advantage. These include the following: (i) lipophilicity is increased (36); (ii) the oxazoline ring nitrogen provides a nonionic ligand which participates in the chelation of ferric

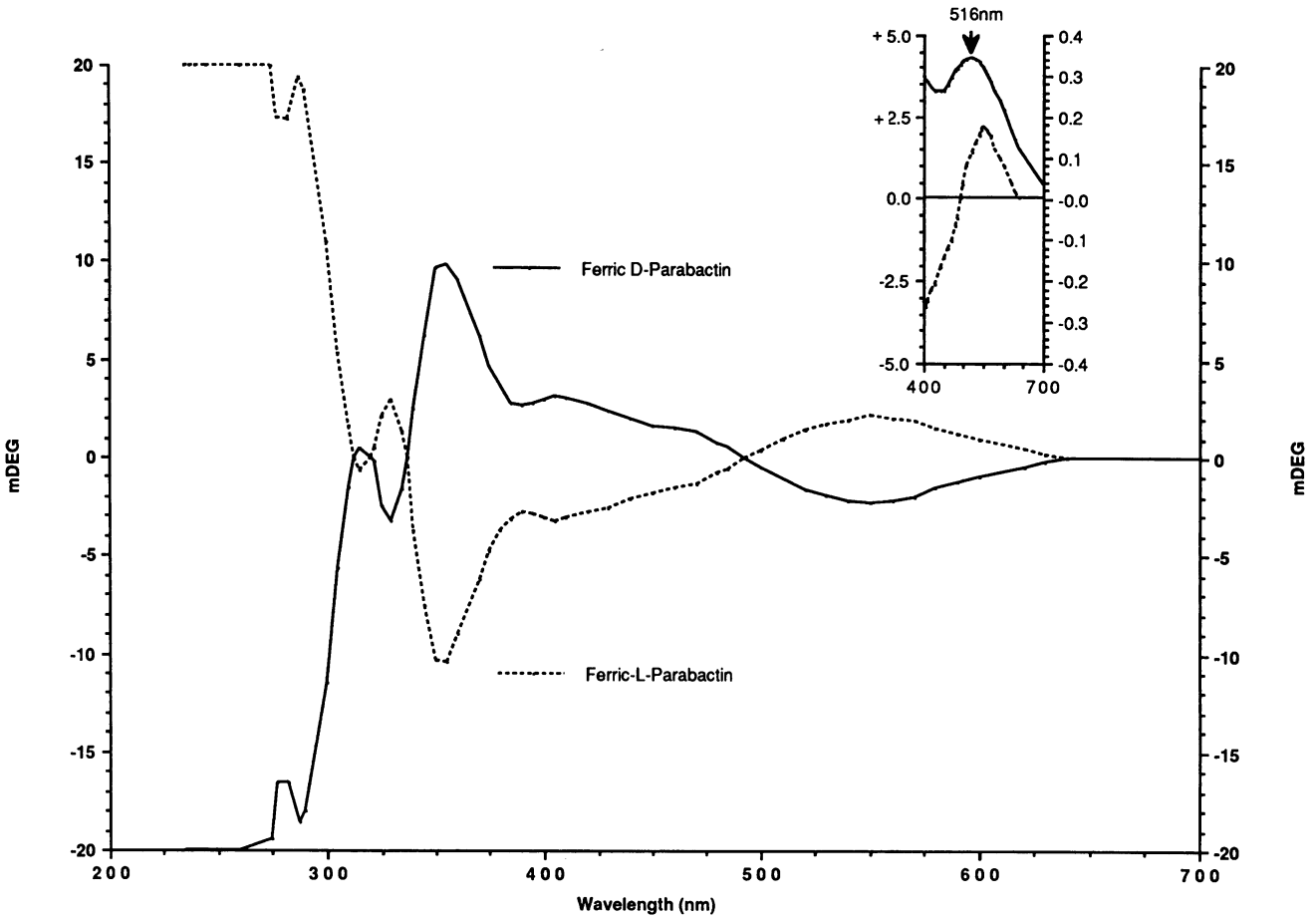

FIG. 4. CD spectra of ferric D- and L-parabactin (100 μM in 100 mM Tris hydrochloride buffer [pH 7.4]). The insert shows the visible absorption spectral band (——; arrow, λ_{max} = 516 nm) and the associated CD band (------, $\Delta\varepsilon$ = +2.2 at 550 nm), demonstrating ferric L-parabactin to be a Λ chelate (see text). The CD spectrum of ferric D-parabactin is an exact mirror image of the CD of ferric L-parabactin. CD spectra of the free ligands, D- and L-parabactin, in methanol are mirror images of one another and indicate opposite configurations of the oxazoline ring. Thus ferric D- and L-parabactin have inverted configurations at three chiral centers: two asymmetric carbons in the oxazoline ring derived from D-(2*R*,3*S*)-threonine (D-parabactin) and L-(2*S*,3*R*)-threonine (L-parabactin) as well as an enantiomeric metal center with Λ (ferric L-parabactin) and Δ (ferric D-parabactin) chelate enantiomers.

ion (34); (iii) compared with the corresponding open-chain threonyl forms, the oxazoline ring may increase conformational rigidity and may result in a much more compact ferric chelate than is otherwise possible (34); and (iv) simple hydrolytic cleavage to open up the oxazoline provides a readily reversible means of altering these and other properties of both the free ligand and the ferric chelate; this may be important in deferration of the chelate, allowing the organism access to the iron (39).

It is notable that neither the presence of an L-oxazoline ring system nor a Λ metal center chirality alone determines whether a chelate can be utilized by *P. denitrificans*. First, this microorganism can accumulate ^{55}Fe from [^{55}Fe]ferric D-parabactin, although not nearly as efficiently as from [^{55}Fe]ferric L-parabactin. The A forms of ferric parabactin (ferric D- and L-parabactin A), in which the oxazoline ring has hydrolyzed to the open-chain threonyl structure, exhibit linear kinetics with a comparatively high K_m (1.4 ± 0.3 μM) and a surprisingly high V_{max} (Fig. 5; Table 1). CD spectra of ferric L-parabactin A (λ_{max} = 522 nm; $\Delta\varepsilon$ = +1.2 at 550 nm; Λ enantiomorph) and ferric D-parabactin A (λ_{max} = 522 nm; $\Delta\varepsilon$ = −1.2 at 550 nm; Δ enantiomorph) are exact mirror images. The marked stereospecific kinetic differences which distinguish ferric D-parabactin from ferric L-parabactin transport are not observed; i.e., iron acquisition from ferric parabactin A is nonstereospecific (Fig. 5).

Net ^{55}Fe accumulation from [^{55}Fe]ferric L-parabactin and [^{55}Fe]ferric L-vibriobactin is strongly inhibited by ferric L-parabactin A (0.5 and 1.0 μM) and, to essentially an equal degree, by ferric D-parabactin A (0.5 and 1.0 μM). These kinetic data indicate a complicated inhibition that does not appear to fit the usual simple models (e.g., competitive, noncompetitive, and uncompetitive). In the reverse inhibition experiment, ^{55}Fe accumulation from the ^{55}Fe(III) chelates of both enantiomers of parabactin A are inhibited by ferric L-parabactin, but again with apparently complicated kinetics. ^{55}Fe accumulation from [^{55}Fe]ferric L-parabactin and [^{55}Fe]ferric parabactin A are not inhibited by ferric D-parabactin (0.5 or 1.0 μM) except at very high concentrations (≥10 μM). Although these inhibition studies are preliminary in the sense of providing mechanistic insights, the phenomena are dramatic, suggesting that ferric parabactin and ferric parabactin A may each be involved in a common pathway. An attractive model consistent with these overall findings involves a stereospecific high-affinity binding step requiring the L-oxazoline ring, followed by a nonstereospe-

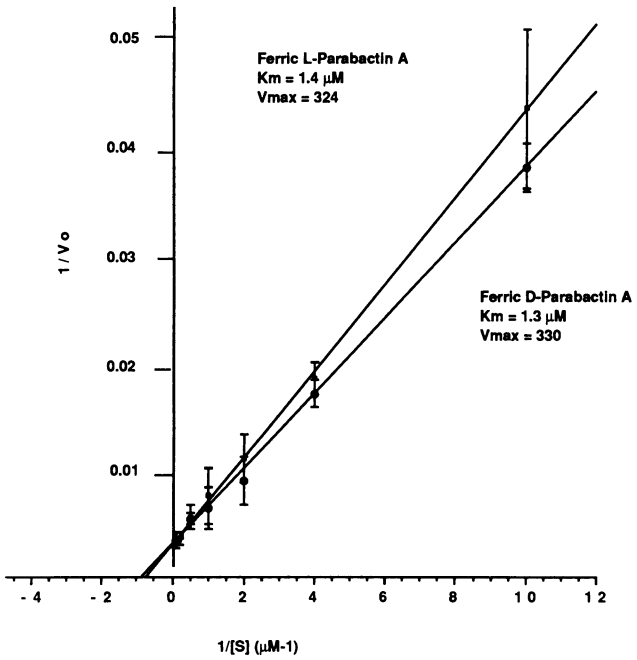

FIG. 5. Lineweaver-Burk plot of kinetic data for ^{55}Fe accumulation from [^{55}Fe]ferric L-parabactin A and [^{55}Fe]ferric D-parabactin A for the concentration range 0.1 μM ≤ [S] ≤ 10 μM. In contrast to the biphasic kinetics exhibited by [^{55}Fe]ferric L-parabactin, these ligands exhibit linear (r = 0.991, 0.996) kinetics with a comparatively high K_m (ca. 1.4 ± 0.3 μM) and high V_{max} (ca. 330 pg-atoms of ^{55}Fe min^{-1} mg of protein^{-1}). Note that the oxazoline ring has hydrolyzed to the open-chain threonyl structure in these A forms. Note also that the marked stereospecificity seen between ferric D- and L-parabactins is absent; i.e., iron acquisition from ferric parabactin A is nonstereospecific. Data are presented as mean and range of two (D-parabactin A) or mean of four (L-parabactin A) determinations and standard deviations (bars) for each [S] = 0.1, 0.25, 0.5, 1.0, 2.0, 5.0, and 10.0 μM.

cific postreceptor processing involving hydrolysis of the oxazoline ring of ferric L-parabactin (E_0' = −0.673 mV; pH 7.0) to the open-chain threonyl structure of ferric parabactin A (E_0' = −0.400 mV; pH 7.0 [39]), from which iron might be much more readily removed, perhaps by a nonstereospecific reductase. We are currently seeking more direct evidence for this model.

A low-affinity iron uptake mechanism acting independently of the high-affinity parabactin iron transport apparatus in *P. denitrificans* has recently been reported (44). The ability of *P. denitrificans* to accumulate iron from a variety of ferric siderophores and related ferric chelates in a nonstereospecific fashion could be due to the presence of a reductase with broad specificity. Such a ferrisiderophore reductase activity has been reported in *Agrobacterium tumefaciens* (28) and *Bacillus subtilis* (27), and a reductase in *Mycobacterium smegmatis* has a K_m for ferrimycobactin estimated to be <4 μM (31), a value similar to the apparent K_ms for iron acquisition from the ferric parabactin A's. Another possible mechanism to explain the loss of stereospecificity might be a ligand exchange mechanism analogous to that proposed for mycobactin-mediated iron transport in *Mycobacterium* spp. (37). Preliminary experiments to assess the magnitude of metal-ligand interchange between ferric parabactin A and parabactin (see Materials and Methods) indicate that it is 4.7% over the 2-min duration of our transport experiments. However, the rates of transport actually observed correspond to about 20% of the metal transferred to the cells in 2 min. Thus, metal-ligand interchange seems insufficient to account for the high V_{max} observed for iron accumulation from ferric parabactin A. Efforts are under way in our laboratory to more completely define the role, if any, of the kinetic lability of metal-ligand complexes and ligand exchange mechanisms and/or membrane reductases in the iron transport apparatus of *P. denitrificans*.

ACKNOWLEDGMENTS

We gratefully acknowledge the excellent technical assistance of Douglas Ward.

This work was supported by Public Health Service grant GM-34897-01 from the National Institutes of Health.

LITERATURE CITED

1. **Anderegg, G. F., L'Eplattenier, and G. Schwarzenbach.** 1963. Hydroxamatkomplexe. II. Die Anwendung der pH-Methode. Helv. Chim. Acta **63**:1400–1408.
2. **Arceneaux, J. E. L., W. B. Davis, D. N. Downer, A. H. Haydon, and B. R. Byers.** 1973. Fate of labeled hydroxamates during iron transport from hydroxamate-iron chelates. J. Bacteriol. **115**: 919–927.
3. **Bergeron, R. J.** 1987. Synthesis and properties of polyamine catecholamide chelators, p. 285–316. *In* G. Winkelmann, D. van der Helm, and J. B. Neilands (ed.), Iron transport in microbes, plants and animals. VCH Verlagsgesellschaft, Weinheim, Federal Republic of Germany.
4. **Bergeron, R. J., J. B. Dionis, G. T. Elliott, and S. J. Kline.** 1985. Mechanism and stereospecificity of the parabactin-mediated iron transport system in *Paracoccus denitrificans*. J. Biol. Chem. **260**:7936–7944.
5. **Bergeron, R. J., J. R. Garlich, and J. S. McManis.** 1985. Total synthesis of vibriobactin. Tetrahedron **41**:507–510.
6. **Bergeron, R. J., and S. J. Kline.** 1982. A short synthesis of parabactin. J. Am. Chem. Soc. **104**:4489–4492.
7. **Bergeron, R. J., and S. J. Kline.** 1984. 300-MHz ^1H NMR study of parabactin and its gallium(III) chelate. J. Am. Chem. Soc. **106**:3089–3098.
8. **Bergeron, R. J., J. S. McManis, J. B. Dionis, and J. R. Garlich.** 1985. An efficient total synthesis of agrobactin and its gallium (III) chelate. J. Org. Chem. **50**:2780–2782.
9. **Bergeron, R. J., N. J. Stolowich, and S. J. Kline.** 1983. Synthesis and solution dynamics of agrobactin A. J. Org. Chem. **48**: 3432–3439.
10. **Bergeron, R. J., W. R. Weimar, and J. B. Dionis.** 1988. Demonstration of ferric L-parabactin-binding activity in the outer membrane of *Paracoccus denitrificans*. J. Bacteriol. **170**: 3711–3717.
11. **Carrano, C. J., and K. N. Raymond.** 1978. Coordination chemistry of microbial iron transport compounds. 10. Characterization of the complexes of rhodotorulic acid, a dihydroxamate siderophore. J. Am. Chem. Soc. **100**:5371–5374.
12. **Cleland, W. W.** 1967. The statistical analysis of enzyme kinetic data Adv. Enzymol. **29**:1–32.
13. **Corbin, J. L., and W. A. Bulen.** 1969. The isolation and identification of 2,3-dihydroxybenzoic acid and 2-N,6-N-di(2,3-dihydroxybenzoyl)-L-lysine formed by iron-deficient *Azotobacter vinelandii*. Biochemistry **8**:757–762.
14. **Cox, C. D., K. L. Rinehart, M. L. Moore, and J. C. Cook.** 1981. Pyochelin: novel structure of an iron-chelating growth promoter for *Pseudomonas aeruginosa*. Proc. Natl. Acad. Sci. USA **78**:4256–4260.
15. **Ecker, D. J., and T. Emery.** 1983. Iron uptake from ferrichrome A and iron citrate in *Ustilago sphaerogena*. J. Bacteriol. **155**: 616–622.
16. **Erecinska, M., C. J. Deutsch, and J. S. Davis.** 1981. Energy coupling to K^+ transport in *Paracoccus denitrificans*. J. Biol. Chem. **256**:278–284.
17. **Findell, P. R., S. M. Torkelson, J. C. Craig, and R. I. Weiner.**

1988. Correlation of α- and β-rotameric forms of 2-substituted octahydrobenzo [*f*]quinoline dopamine congeners with high and low affinity states of the anterior pituitary dopamine receptor and prolactin inhibition. Mol. Pharmacol. **33**:78–83.

18. **Frost, G. E., and H. Rosenberg.** 1973. The inducible citrate-dependent iron uptake system in *Escherichia coli* K12. Biochim. Biophys. Acta **330**:90–101.
19. **Griffiths, G. L., S. P. Sigel, S. M. Payne, and J. B. Neilands.** 1984. Vibriobactin, a siderophore from *Vibrio cholerae*. J. Biol. Chem. **259**:383–385.
20. **Hoe, M., B. J. Wilkinson, and M. S. Hindahl.** 1985. Outer membrane proteins induced upon iron deprivation of *Paracoccus denitrificans*. Biochim. Biophys. Acta **813**:338–342.
21. **Holman, G. D., A. L. Busza, E. J. Pierce, and W. D. Rees.** 1981. Evidence for negative cooperativity in human erythrocyte sugar transport. Biochim. Biophys. Acta **649**:503–514.
22. **Huschka, H., H. U. Naegeli, H. Leuenberger-Ryf, W. Keller-Schierlein, and G. Winkelmann.** 1985. Evidence for a common siderophore transport system but different siderophore receptors in *Neurospora crassa*. J. Bacteriol. **162**:715–721.
23. **Isied, S. S., G. Kuo, and K. N. Raymond.** 1976. Coordination isomers of biological iron transport compounds. V. The preparation and chirality of the chromium[III] enterobactin complex and model tris(catechol)chromium [III] analogues. J. Am. Chem. Soc. **98**:1763–1766.
24. **Jalal, M. A. F., M. B. Hossain, D. van der Helm, J. Sanders-Loehr, L. A. Actis, and J. H. Crosa.** 1989. Structure of anguibactin, a unique plasmid-related bacterial siderophore from the fish pathogen *Vibrio anguillarum*. J. Am. Chem. Soc. **111**: 292–296.
25. **Keller-Schierlein, W., and V. Prelog.** 1961. Stoffwechselprodukte von Actinomyceten. 30. Uber das ferrioxamin E; ein beitrag zur konstitution des nocardamins. Helv. Chim. Acta **44**:1981–1985.
26. **Lammers, P. J., and J. Sanders-Loehr.** 1982. Active transport of ferric schizokinen in *Anabaena* sp. J. Bacteriol. **151**:288–294.
27. **Lodge, J. S., C. G. Gaines, J. E. L. Arceneaux, and B. R. Byers.** 1980. Non-hydrolytic release of iron from ferrienterobactin analogues by extracts of *Bacillus subtilis*. Biochem. Biophys. Res. Commun. **97**:1291–1295.
28. **Lodge, J. S., C. G. Gaines, J. E. L. Arceneaux, and B. R. Byers.** 1982. Ferrisiderophore reductase activity in *Agrobacterium tumefaciens*. J. Bacteriol. **149**:771–774.
29. **Lowry, O. H., N. J. Rosebrough, A. L. Farr, and R. J. Randall.** 1951. Protein measurement with the Folin phenol reagent. J. Biol. Chem. **193**:265–275.
30. **Markwel, M. K., S. M. Haas, L. L. Bieber, and N. E. Tolbert.** 1978. A modification of the Lowry procedure to simplify protein determination in membrane and lipoprotein samples. Anal. Biochem. **87**:206–210.
31. **McCready, K. A., and C. Ratledge.** 1979. Ferrimycobactin reductase activity from *Mycobacterium smegmatis*. J. Gen. Microbiol. **113**:67–72.
32. **Muller, G., and K. N. Raymond.** 1984. Specificity and mechanism of ferrioxamine-mediated iron transport in *Streptomyces pilosus*. J. Bacteriol. **160**:304–312.
33. **Negrin, R. S., and J. B. Neilands.** 1978. Ferrichrome transport in inner membrane vesicles of *Escherichia coli* K12. J. Biol. Chem. **253**:2339–2342.
34. **Neilands, J. B., T. Peterson, and S. A. Leong.** 1980. High affinity iron transport in microorganisms. ACS Symp. Ser. **140**:263–278.
35. **Ong, S. A., T. Peterson, and J. B. Neilands.** 1979. Agrobactin, a siderophore from *Agrobacterium tumerfaciens*. J. Biol. Chem. **254**:1860–1865.
36. **Peterson, T., and J. B. Neilands.** 1979. Revised structure of a catecholamide spermidine siderophore from *Paracoccus denitrificans*. Tetrahedron Lett. **50**:4805–4808.
37. **Ratledge, C., P. V. Patel, and J. Mundy.** 1982. Iron transport in *Mycobacterium smegmatis*: the location of mycobactin by electron microscopy. J. Gen. Microbiol. **128**:1559–1565.
38. **Raymond, K. N., K. Abu-Dari, and S. R. Sofen.** 1980. Stereochemistry of microbial iron transport compounds. ACS Symp. Ser. **119**:133–167.
39. **Robinson, J. P., and J. V. McArdle.** 1981. Electrochemistry of ferric complexes of parabactin and parabactin A. J. Inorg. Nucl. Chem. **43**:1951–1953.
40. **Rosenberg, H.** 1979. Bacterial iron transport. Methods Enzymol. **56**:388–394.
41. **Snow, G. A.** 1970. Mycobactins: iron-chelating growth factors from mycobacteria. Bacteriol. Rev. **34**:99–125.
42. **Tait, G. T.** 1975. The identification and biosynthesis of siderochromes formed by *Micrococcus denitrificans*. Biochem. J. **146**:191–204.
43. **Wang, C. C., and A. Newton.** 1971. An additional step in the transport of iron as defined by the tonB locus of *Escherichia coli* K12. J. Biol. Chem. **246**:2147–2151.
44. **Wee, S., S. Hardesty, M. V. V. S. Madiraju, and B. J. Wilkinson.** 1988. Iron-regulated outer membrane proteins and non-siderophore mediated iron acquisition by *Paracoccus denitrificans*. FEMS Microbiol. Lett. **51**:33–36.
45. **Wiebe, C., and G. Winkelmann.** 1975. Kinetic studies on the specificity of chelate-iron uptake in *Aspergillus*. J. Bacteriol. **123**:39–50.
46. **Winkelmann, G.** 1974. Metabolic products of microorganisms: uptake of iron by *Neurospora crassa*. Arch. Microbiol. **98**: 39–50.
47. **Winkelmann, G.** 1979. Evidence for stereospecific uptake of iron chelates in fungi. FEBS Lett. **97**:43–46.
48. **Wong, G. B., M. J. Kappel, K. N. Raymond, B. Matzanke, and G. Winkelmann.** 1983. Coordination chemistry of microbial iron transport compounds. 24. Characterization of coprogen and ferricrocin, two ferric hydroxamate siderophores. J. Am. Chem. Soc. **105**:810–815.